

OPTICAL DESIGN OF AVF WEAK-FOCUSING ACCELERATOR

C. Hori*, T. Aoki, T. Hae, T. Seki, K. Hiramoto, Hitachi, Ltd., Hitachi, Japan

Abstract

A trend in proton beam therapy systems is downsizing their footprints. A larger main magnetic field for the downsizing, however, requires a septum magnet to generate a larger magnetic field for beam extraction. In order to relax the specification of the septum magnet, we consider an azimuthally varying field (AVF) weak-focusing accelerator. The magnetic fields of its hills and valleys can be designed while maintaining the average magnetic fields over the design orbits. Thus, by locating the septum magnet near one of the valleys, the specification is relaxed while keeping the footprint of the accelerator. In this study, we show an optical design of an AVF weak-focusing accelerator with cotangential orbits. The magnetic field in the valleys is smaller than the average magnetic field over the maximum energy orbit by 0.2 T. We evaluate gradient magnetic fields required for beam extraction and find the possibility of variable energy extraction by the static gradient fields.

INTRODUCTION

A trend in proton beam therapy (PBT) systems is downsizing their footprints. We have proposed a compact accelerator for PBT with cotangential orbits [1, 2]. Figure 1 shows a schematic of the accelerator. Its concept is to achieve both compactness and variable energy extraction. For compactness, a superconducting magnet which generates a weak-focusing magnetic field of approximately 4-5 T and an RF cavity which can modulate its frequency are applied. For variable energy extraction, the orbits are not concentric but cotangential like the classical microtron, and an RF kicker and gradient fields (generated by a peeler and a regenerator) are combined. Due to the characteristic orbit configuration, there is small turn separation region on one side, where the RF kicker is installed. Each orbit between 70 MeV and 235 MeV passes through the RF kicker. By turning on the RF kicker, the beam trajectory is moved toward the outside of the circulating region. The beam moved by the RF kicker is eventually affected by the gradient magnetic fields generated by the peeler and the regenerator. The gradient magnetic fields bring about 2/2 resonance, and the beam arrives at the entrance of the extraction channel. Along the extraction channel, septum magnetic fields are applied to extract the beam from the accelerator.

A larger main magnetic field requires septum magnets to generate larger magnetic fields for extraction. Since the proposed accelerator is designed to extract low energy (approximately of 70 MeV) beams, it requires the septum magnets to generate even larger magnetic fields compared with cyclotrons and synchrocyclotrons. Among the septum magnets, the first septum magnet, which is located at the entrance

of the extraction channel, is under the severest conditions. Hence, we considered a new idea to relax the specification of the first septum magnet.

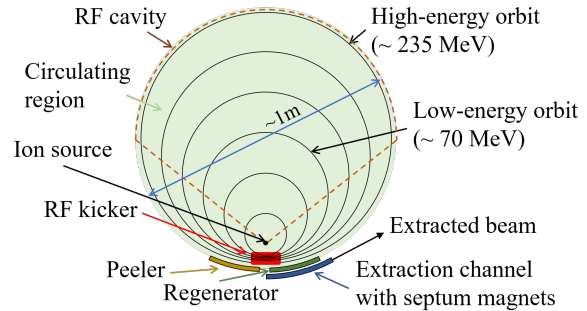


Figure 1: Schematic of compact accelerator.

AVF WEAK-FOCUSING ACCELERATOR

We denote the fringe magnetic field at the entrance of the extraction channel by B_f , and the first septum magnetic field by $-\delta B$. Then the curvature radius of the beam at the entrance is given by

$$\rho(K) = \frac{\sqrt{K(K + 2E_0)}}{cq(B_f - \delta B)}, \quad (1)$$

where c denotes the speed of light, and q , E_0 , and K denote charge, rest energy, and kinetic energy of the beam, respectively. We denote the maximum kinetic energy and the average main magnetic field over the maximum kinetic energy orbit by K_M and B_M , respectively. In order to extract the beam with its energy of K , $\rho(K)$ has to be larger than ρ_M , where ρ_M is given by

$$\rho_M = \frac{\sqrt{K_M(K_M + 2E_0)}}{cqB_M}. \quad (2)$$

If B_f is reduced, δB is also reduced while $\rho(K)$ maintained. The easiest approach to reduce B_f is to reduce B_M . However, if B_M is reduced, not only B_f is reduced, but also ρ_M is increased, indicating a larger footprint of the accelerator and larger $\rho(K)$ for extraction. Hence for relaxing the specification of the first septum magnet, B_f should be reduced without reducing B_M . To satisfy this condition, we consider an azimuthally varying field (AVF) weak-focusing accelerator. By locating the extraction channel near one of the valleys, B_f at the extraction channel is reduced while B_M maintained.

The AVF field is normally applied to cyclotrons to satisfy both isochronism and stable betatron motion. Since isochronism requires a magnetic field to increase with radius, the average magnetic fields of usual AVF cyclotrons increase

Content from this work may be used under the terms of the CC BY 3.0 licence (© 2019). Any distribution of this work must maintain attribution to the author(s), title of the work, publisher, and DOI

* chishin.hori.cj@hitachi.com

with radius. In contrast to the usual AVF cyclotrons, the proposed accelerator does not require isochronism, since the frequency of the RF cavity is modulated. The average magnetic field should decrease with radius in accordance with the weak-focusing principle.

OPTICAL DESIGN

Method

A special tool is required to design the optics of the AVF weak-focusing accelerator with cotangential orbits. We developed a design tool based on the transfer matrix method for an isochronous accelerator with cotangential orbits [3]. We have applied this tool to design the optics of the AVF weak-focusing accelerator. Since it does not require isochronism, we give the average magnetic field \bar{B} as the function of the beam velocity β by

$$\bar{B}(\beta) = \begin{cases} -b_1 \left(\frac{\beta}{\beta_M}\right)^{p_1} + B_{\max} & 0 \leq \beta \leq \beta_m \\ b_2 \left[1 - \left(\frac{\beta}{\beta_M}\right)^{p_2}\right] + B_{\min} & \beta_m \leq \beta \leq \beta_M \end{cases}, \quad (3)$$

where p_1 , p_2 , B_{\max} , B_{\min} , and β_m are adjustable parameters, and β_M is determined by K_M . The other parameters b_1 and b_2 are determined by the condition that \bar{B} and its first derivative with respect to β are continuous at $\beta = \beta_m$. We note that B_{\max} and B_{\min} are maximum and minimum of \bar{B} , respectively. Hence the magnetic field at the hills is larger than B_{\max} , and the magnetic field at the valleys is smaller than B_{\min} .

Design Orbits and Tunes

In the following, we show an example of the optical design, where K_M and B_M are fixed at 235 MeV and 4.5 T, respectively.

Figure 2 shows the design orbits and the magnetic fields. The magnetic field at the hills is 5.04 T, while the magnetic field at the valleys is 4.28 T, which is smaller than B_M by approximately 0.2 T. This difference is expected to contribute to reducing the first septum magnet field.

Figure 3 shows the horizontal and the vertical tunes, which are denoted by ν_h and ν_v , respectively. The solid curves indicate design tunes by the tool, while the plotted symbols are obtained by the beam tracking simulation code GPT [4]. The design tunes and the tracking simulation results agree within the accuracy of 10%. Since the tool models the magnetic fields by the hard edge model, it is not applicable to the low energy region. Hence the tunes are evaluated above the energy of 10 MeV. In order to utilize $2/2$ resonance by the peeler and regenerator for extraction, the horizontal tunes are designed to be more than 0.95 in all energy regions. The vertical tunes are designed to avoid the second resonance line $\nu_v = 0.5$.

Figure 4 shows the tune diagram, where the resonance lines up to the fourth order are drawn. The Walkinshaw resonance ($\nu_h = 2\nu_v$) is avoided.

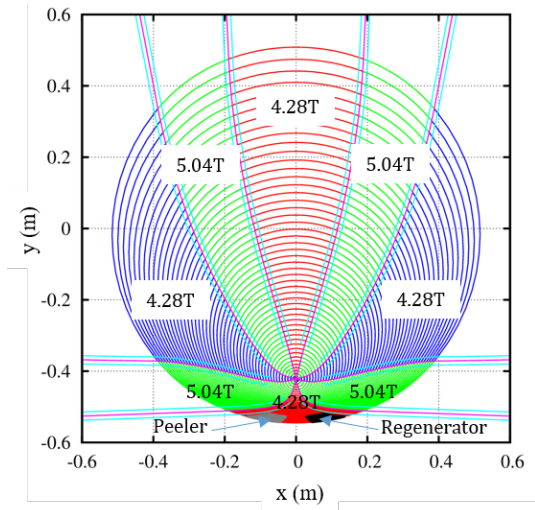


Figure 2: Design orbits and magnetic fields.

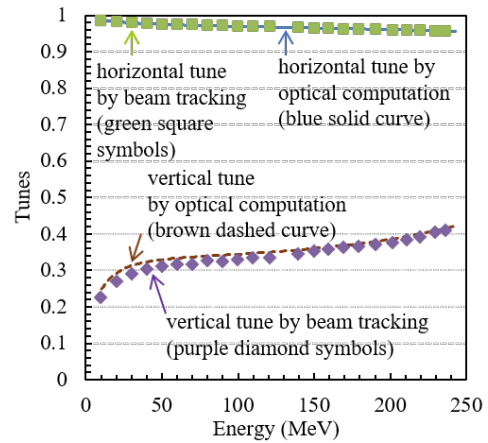


Figure 3: Betatron frequencies (tunes).

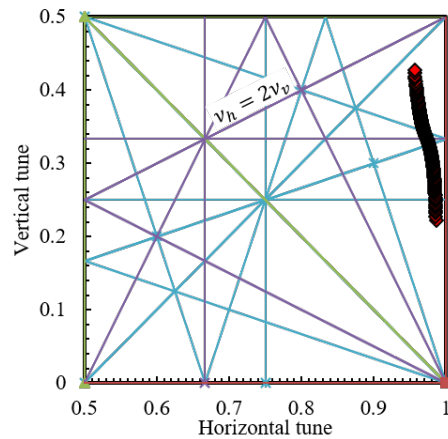


Figure 4: Tune diagram.

Gradient Magnetic Fields for Extraction

As is shown in Fig. 1, the peeler and the regenerator are located outside the circulating region. In order to estimate required strengths of those fields, however, the peeler and the

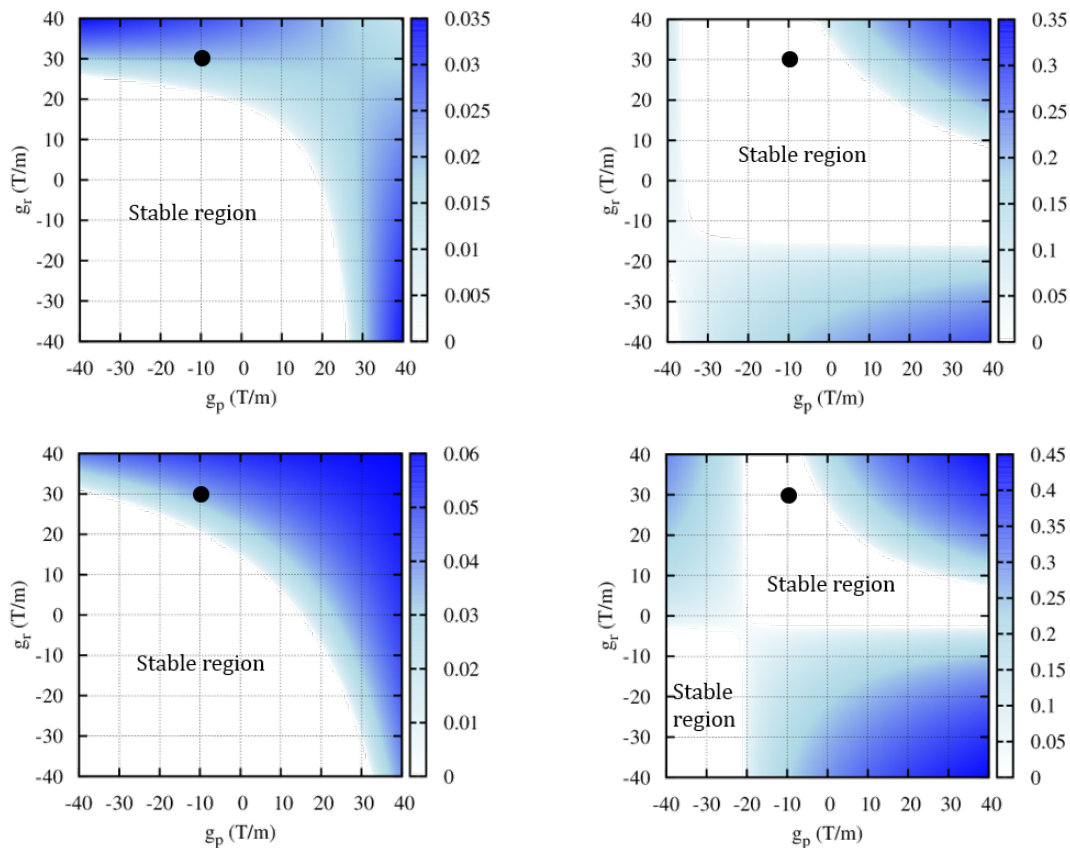


Figure 5: Imaginary parts of tunes. Upper left and upper right are horizontal and vertical tunes at 67.8 MeV, respectively. Lower left and lower right are horizontal and vertical tunes at 236.3 MeV, respectively.

regenerator are assumed to be in the valley shown in Fig. 2 for simplicity, and the imaginary parts of the tunes are evaluated by the transfer matrix method. Figure 5 shows color maps of the imaginary parts, where g_p and g_r denote the strengths of the peeler and the regenerator, respectively. The betatron motion becomes unstable when the corresponding tune has a nonzero imaginary part. For extraction, $\text{Im}(\nu_h)$ has to be larger than zero, while $\text{Im}(\nu_v)$ has to remain zero. For example, the point of $(g_p, g_r) = (-10, 30)$, which is indicated by the black circle symbol in Fig. 5, satisfies that condition for both 67.8 MeV and 236.3 MeV. This result indicates the possibility of static gradient magnetic fields for variable energy extraction.

CONCLUSION

We considered the AVF weak-focusing accelerator with cotangential orbits for proton beam therapy to achieve both compactness and variable energy extraction. By locating the first septum magnet outside the valley, its specification was relaxed. The possibility of variable energy extraction by

the static gradient magnetic fields was indicated. We noted that the idea of the AVF weak-focusing accelerator would be applicable to axisymmetric synchrocyclotrons.

REFERENCES

- [1] T. Aoki, T. Hae, C. Hori, T. Seki, Y. Nakashima, and F. Ebina, “Concept of frequency modulated variable-energy accelerator”, in *Proc. 14th Annual Meeting of Particle Accelerator Society of Japan (PASJ'17)*, Sapporo, Japan, Aug. 1-3, 2017, paper THOL02, pp. 150-154.
- [2] T. Hae *et al.*, “Compact cotangential orbits accelerator for proton therapy”, in *Proc. 22nd Int. Conf. Cyclotrons and their Applications (CYC'19)*, Cape Town, South Africa, Sep. 22-27, 2019, paper TUP037, this conference.
- [3] C. Hori, T. Aoki, and T. Seki, “Variable-energy isochronous accelerator with cotangential orbits for proton beam therapy”, *Nucl. Instrum. Methods Phys. Res., Sect. A*, vol. 922, pp. 352-356, Apr. 2019. doi:10.1016/j.nima.2019.01.005
- [4] GPT, <http://www.pulsar.nl/gpt/index.html>